

Generating superpositions of higher-order Bessel beams

Ruslan Vasilyeu¹, Angela Dudley^{2,3}, Nikolai Khilo¹, and Andrew Forbes^{2,3,*}

¹ B.I. Stepanov Institute of Physics of NAS of Belarus, Nezalezhnasti Ave., 68, 220072 Minsk, Belarus

² School of Physics, University of KwaZulu-Natal, Private Bag X54001, Durban 4000, South Africa

³ CSIR National Laser Centre, PO Box 395, Pretoria 0001, South Africa

*ajforbes1@csir.co.za

Abstract: We report the first experimental generation of the superposition of higher-order Bessel beams, by means of a spatial light modulator (SLM) and a ring slit aperture. We present illuminating a ring slit aperture with light which has an azimuthal phase dependence, such that the field produced is a superposition of two or more higher-order Bessel beams. The experimentally produced fields are in good agreement with those calculated theoretically. The significance of these fields is that even though one is able to generate fields which carry zero orbital angular momentum, a rotation in the field's intensity profile as it propagates is observed.

©2009 Optical Society of America

OCIS codes: (140.3300) Laser Beam Shaping; (080.4865) Optical Vortices.

References and links

1. J. Durmin, "Exact solutions for nondiffracting beams. I. The scalar theory," *J. Opt. Soc. Am. A* **4**(4), 651–654 (1987).
 2. J. Durmin, J. J. Miceli, Jr., and J. H. Eberly, "Diffraction-free beams," *Phys. Rev. Lett.* **58**(15), 1499–1501 (1987).
 3. R. M. Herman, and T. A. Wiggins, "Production and uses of diffractionless beams," *J. Opt. Soc. Am. A* **8**(6), 932–942 (1991).
 4. J. Arlt, and K. Dholakia, "Generation of high-order Bessel beams by use of an axicon," *Opt. Commun.* **177**(1-6), 297–301 (2000).
 5. J. Turunen, A. Vasara, and A. T. Friberg, "Holographic generation of diffraction-free beams," *Appl. Opt.* **27**(19), 3959–3962 (1988).
 6. A. Vasara, J. Turunen, and A. T. Friberg, "Realization of general nondiffracting beams with computer-generated holograms," *J. Opt. Soc. Am. A* **6**(11), 1748–1754 (1989).
 7. H. S. Lee, B. W. Stewart, K. Choi, and H. Fenichel, "Holographic nondiffracting hollow beam," *Phys. Rev. A* **49**(6), 4922–4927 (1994).
 8. G. Indebetouw, "Nondiffracting optical fields: some remarks on their analysis and synthesis," *J. Opt. Soc. Am. A* **6**(1), 150–152 (1989).
 9. J. A. Davis, E. Carcole, and D. M. Cottrell, "Nondiffracting interference patterns generated with programmable spatial light modulators," *Appl. Opt.* **35**(4), 599–602 (1996).
 10. J. A. Davis, E. Carcole, and D. M. Cottrell, "Intensity and phase measurements of nondiffracting beams generated with a magneto-optic spatial light modulator," *Appl. Opt.* **35**(4), 593–598 (1996).
 11. C. Paterson, and R. Smith, "Higher-order Bessel waves produced by axicon-type computer-generated holograms," *Opt. Commun.* **124**(1-2), 121–130 (1996).
 12. J. H. McLeod, "The axicon: a new type of optical element," *J. Opt. Soc. Am.* **44**(8), 592–597 (1954).
 13. D. McGloin, G. C. Spalding, H. Melville, W. Sibbett, and K. Dholakia, "Three-dimensional arrays of optical bottles," *Opt. Commun.* **225**(4-6), 215–222 (2003).
 14. D. McGloin, V. Garcés-Chávez, and K. Dholakia, "Interfering Bessel beams for optical micromanipulation," *Opt. Lett.* **28**(8), 657–659 (2003).
 15. T. A. King, W. Hogervorst, N. S. Kazak, N. A. Khilo, and A. A. Ryzhevich, "Formation of higher-order Bessel light beams in biaxial crystals," *Opt. Commun.* **187**(4-6), 407–414 (2001).
 16. V. V. Kotlyar, S. N. Khonina, R. V. Skidanov, and V. A. Soifer, "Rotation of laser beams with zero of the orbital angular momentum," *Opt. Commun.* **274**(1), 8–14 (2007).
 17. L. Burger, and A. Forbes, "Kaleidoscope modes in large aperture Porro prism resonators," *Opt. Express* **16**(17), 12707–12714 (2008).
-

1. Introduction

There is an extensive body of literature on generating zero order and higher-order Bessel beams. Durnin [1] first discovered a set of solutions for the free-space Helmholtz equation which are propagation-invariant and are mathematically described by Bessel functions. Even though it is not possible to experimentally generate an ideal Bessel beam, as it contains an infinite number of rings over an infinite area resulting in the beam carrying infinite energy, an approximation can be realized in the form of Bessel-Gauss beams that propagate diffraction-free over a finite distance [2–11].

Zero-order Bessel beams possess a bright central maximum, while the higher-orders have a dark central vortex, which propagates over an extended distance in a diffraction-free manner. Zero order Bessel beams can be generated by illuminating a ring slit aperture, placed in the back focal plane of a lens, with a plane wave [2]. Refractive optical elements, such as axicons [3,4,12] and diffractive optical elements such as computer generated holograms [5,6,9–11,13], have been used to generate both zero and higher-order Bessel beams. In particular it has been shown that it is possible to create a superposition of high-order Bessel beams by extending the results in ref [4]. to illuminate an axicon with a superposition of Laguerre-Gauss (LG) beams [14]. This overcomes the problem of creating a Bessel beam interferometer, but requires the creation of high order LG beams on demand in the laboratory.

In this paper we extend Durnin’s original experiment to create a ring slit aperture in the Fourier plane with multiple azimuthal phase components at varying radial distances, thereby producing a superposition of higher-order Bessel beams as the output. The concept is illustrated graphically in Fig. 1, where two separable azimuthal phase components, namely $\exp(im\phi)$ and $\exp(in\phi)$, are combined to produce a superposition of an m^{th} order and n^{th} order Bessel beam.

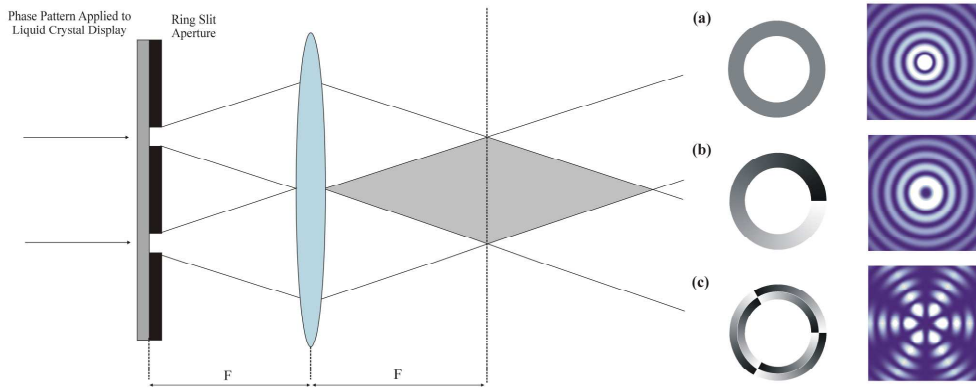


Fig. 1. Extension of Durnin’s ring slit experiment [2]. (b) and (c): Illuminating the ring slit aperture with a beam whose angular spectrum carries an azimuthally varying phase generates higher-order and superpositions of higher-order Bessel beams.

2. Theory

An ideal Bessel beam (in cylindrical coordinates, (r, ϕ, z)) is characterized by a transverse component of the electrical field:

$$E(r, \phi, z) = a_0 J_m(k_r r) \exp[i(k_z z + m\phi)], \quad (1)$$

where J_m is the m^{th} order Bessel function, while k_z and k_r are the longitudinal and transverse wave numbers respectively, with $k_r = k_0 \sin \alpha$, $k_z = k_0 \cos \alpha$, and $k_0 = 2\pi/\lambda$; λ is the wavelength and α is the opening angle of the cone on which the waves traverse. It is seen from Eq. (1) that higher-order Bessel beams ($|m| > 1$) have an azimuthal phase dependence, $\exp(im\phi)$, on the beam axis and hence have a nondiffracting dark core.

Consider the ideal case where an incident Gaussian beam is transformed to a ring field, with radius R and width 2Δ , by a ring slit aperture. If the ring slit aperture is divided equally in the radial direction to yield two azimuthal phase components, denoted by azimuthal mode index m and n in the inner and outer rings respectively, then the resulting superposition is calculated from the Kirchoff–Huygens diffraction integral

$$A_{m,n}(r, \phi, z) = \frac{-i}{\lambda z} \int_0^{2\pi} \int_{R-\Delta}^{R+\Delta} \tau(r, \phi) \exp \left[i \frac{k_0}{2f} \left(1 - \frac{z}{f} \right) r_1^2 \right] \exp \left[-i \frac{k_0 r r_1}{f} \cos(\phi_1 - \phi) \right] r_1 dr_1 d\phi_1 \quad (2)$$

with the transmission function of the ring slit aperture given by:

$$\tau(r, \phi) = \begin{cases} \exp(im\phi), & R \geq r \geq (R - \Delta) \\ \exp(in\phi), & R \leq r \leq (R + \Delta) \end{cases} \quad (3)$$

The total field may be decomposed into the contribution resulting from the inner ring (azimuthal mode index m) and the outer ring (azimuthal mode index n), given respectively as:

$$A_m(r, \phi, z) = \frac{-ik_0}{f} \int_{R-\Delta}^R i^m \exp(im\phi) J_m \left(\frac{k_0 r r_1}{f} \right) \exp \left[-\frac{r_1^2}{w^2} + \frac{ik_0 r_1^2}{2f} \left(1 - \frac{z}{f} \right) \right] r_1 dr_1, \quad (4)$$

$$A_n(r, \phi, z) = \frac{-ik_0}{f} \int_R^{R+\Delta} i^n \exp(in\phi) J_n \left(\frac{k_0 r r_1}{f} \right) \exp \left[-\frac{r_1^2}{w^2} + \frac{ik_0 r_1^2}{2f} \left(1 - \frac{z}{f} \right) \right] r_1 dr_1, \quad (5)$$

so that the resulting field may be expressed as a superposition of the form:

$$A_{m,n}(r, \phi, z) = A_m(r, \phi, z) + A_n(r, \phi, z). \quad (6)$$

Specifically, the superposition of an m^{th} order Bessel beam with its mirror image ($-m^{\text{th}}$ order Bessel beam), results in a spatial intensity pattern of $2m$ spots arranged on the circumference of a ring (with an angular offset depending on whether m is even/odd):

$$A_{m,-m}(r, \phi, z) = J_m(k_r r) \sin(m\phi) \exp(ik_z z). \quad (7)$$

Such a field carries no orbital angular momentum (OAM), although we will show later that there is a rotation in the field structure when it is created with a two-component ring structure as described by Eq. (3).

3. Experimental methodology and results

Our experimental setup is shown in Fig. 2. A HeNe laser ($\lambda \sim 633$ nm) was expanded through a $15 \times$ telescope ($f_1 = 10$ mm, $f_2 = 150$ mm) before illuminating a suitable ring slit aperture ($R = 3$ mm and $2\Delta = 150$ μm). The resulting field was relay imaged to the plane of the liquid crystal display with a $0.75 \times$ telescope ($f_3 = 100$ mm, $f_4 = 75$ mm). The liquid crystal on silicon device used for imparting the azimuthal phase variation on the field was a spatial light modulator (SLM) (Holoeye, HEO1080P) with 1920×1080 pixels of pitch 8 μm and calibrated for a 2π phase shift at ~ 633 nm. The angle of incidence on the SLM was kept as low as possible, typically $< 10^\circ$ in the experiment. Larger angles would cause a phase error as a result of the increased path length in the liquid crystal medium. The Fourier transform field (after the $f_5 = 200$ mm lens) was magnified with a $10 \times$ objective and detected on a CCD camera (Spiricon, USB L130); both the objective and camera were positioned on a translation stage in order to investigate the propagation of the resulting field. An interferometer, denoted by the shaded box, was introduced in the experimental setup as needed to reveal the phase dislocations in the superposition fields [15].

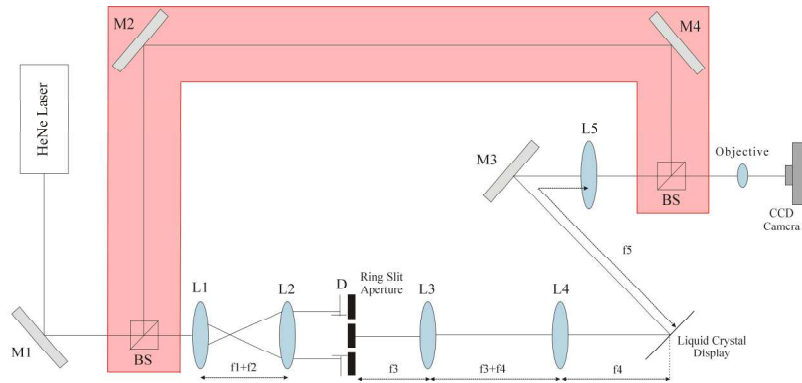


Fig. 2. The experimental design for generating a superposition of two higher-order Bessel beams. The interferometer used to interfere the field produced at the Fourier plane with a plane wave is denoted in the shaded overlay. (M: mirror; BS: beam-splitter; L: lens and D: diaphragm). Note the distances and angles are not to scale.

In such a system alignment of the ring field and the phase pattern is of course important. Careful alignment using standard micrometer adjustable translation stages was done prior to the azimuthally varying patterns loaded onto the SLM. Thereafter the scaling of the image relative to the SLM was sufficient to maintain the alignment for the experiments to follow. Results of our superposition fields, as viewed in the far field, are shown in Fig. 3.

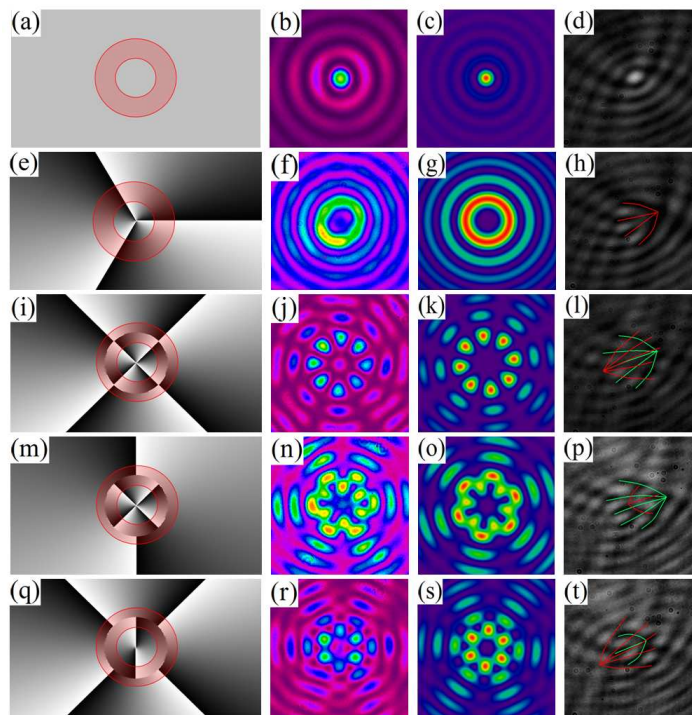


Fig. 3. The columns from left to right represent the phase patterns applied to the liquid crystal display of the SLM, the observed intensity distribution of the superposition, the theoretical prediction, and interference pattern of the superposition field and a plane wave, respectively. Data is shown for (a) – (d): A_0 , (e) – (h): A_3 , (i) – (l): $A_{4,4}$, (m) – (p): $A_{2,4}$, and (q) – (t): $A_{4,2}$. The illuminated ring slit is shown as a shaded overlay on the phase pattern.

With no azimuthally varying phase (Fig. 3(a)) the resulting pattern (Fig. 3(b)) is the well known zeroth order Bessel beam, while with a single azimuthal component to the phase

(Fig. 3(e)) the corresponding higher-order Bessel beam is reproduced (Fig. 3(f)). The vortex nature of this field is confirmed in the interferogram of Fig. 3(h) where three dislocations are noted in the fork-like pattern. When more than one azimuthal component is introduced to the SLM, the resulting pattern becomes more complex. Nevertheless, in all cases the theoretical prediction is in excellent agreement with that measured experimentally, as is easily noted by comparison of columns two and three in Fig. 3 for any given row. As noted earlier in the theory section, when the orders of the two azimuthal phases are equal but opposite in sign, a petal-like pattern is produced. This is evident in Figs. 3(j) and 3(k) for both the measured and calculated fields respectively. Note also that the phase patterns used for a given azimuthal component are not required to extend to the origin. Due to the azimuthally varying phase which is imparted to the angular spectrum of the ring field, the resulting fields possess vortices which can be investigated by interference with the Gaussian source [15]. Since the beam size of the Gaussian beam is large in comparison to the Bessel field in the Fourier plane, the wavefront of the Gaussian field can be assumed to be flat, similar to a plane wave. The interference patterns obtained contain two overlapping forks, illustrating the presence of two higher-order Bessel fields. The number of dislocations or spaces between the ‘fork-prongs’ conveys the order of the Bessel fields involved in the superposition. The direction of the ‘fork-prongs’ illustrates that the two higher-order Bessel fields are of opposite handedness.

While we have demonstrated the concept here with the superposition of two Bessel fields, it is possible in principle to extend this to any number of azimuthal components. Figure 4 shows a three-component superposition, with azimuthal mode indices (outer to inner radii) of -3 , 0 and 3 respectively. As expected, the theoretical predictions are in excellent agreement with experiment. However, superpositions of more than three higher-order Bessel beams were not attempted due to the restricting dimensions of the ring slit aperture and the resolution of our SLM.

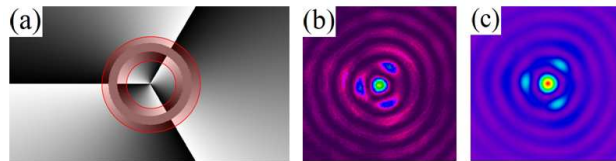


Fig. 4. (a) Phase pattern applied to the liquid crystal display. The shaded overlay denotes the section of the phase pattern which is illuminated by the ring field. (b) The experimental beam cross-section of the field produced at the Fourier plane. (c) It is in good agreement with the calculated field.

Apart from investigating the field produced at the Fourier plane, the propagation of these fields was also considered. Experimental images of the intensity profile of the produced field were captured along its propagation. A schematic of this is illustrated in Fig. 5. In studying these images, some of which are presented as video clips in Fig. 6, it is evident that the intensity profile containing the highest amount of energy occurs half way along the field’s propagation. For our experimental setup this occurs at approximately 205 mm after L5. This is in close agreement with the theoretical prediction that the intensity profile containing the highest amount of energy occurs at the focal length of the Fourier transforming lens ($f_5 = 200$ mm).

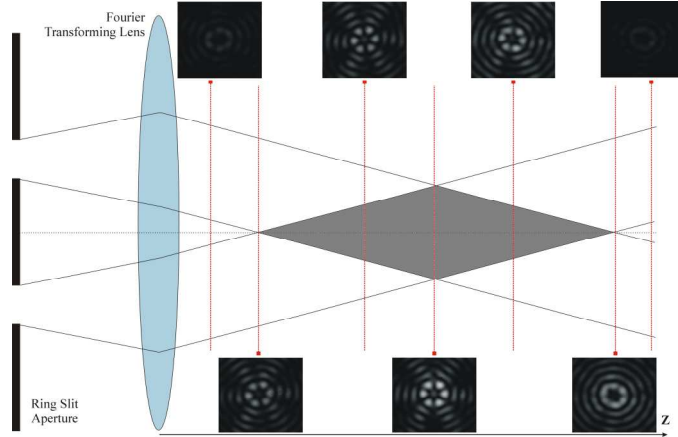


Fig. 5. Images of the intensity profile of the experimentally produced field $A_{3,3}$ captured at intervals along its propagation. The grey area denotes the region in which the Bessel field exists.

In the video clips in Fig. 6 one also notes a rotation of the field as it propagates. This is a surprising phenomenon as in both cases an m^{th} order Bessel beam is superimposed with a $-m^{\text{th}}$ order Bessel beam, resulting in the field carrying no orbital angular momentum (as seen from Eq. (7)). However, one witnesses a rotation in the cross-section intensity distribution of the beam.

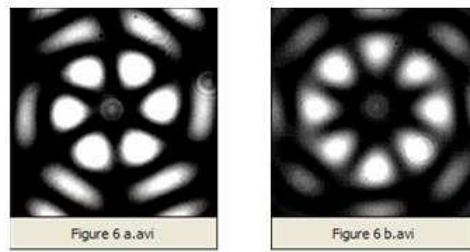


Fig. 6. Video clips containing experimental images for fields (left): $A_{3,3}$ (media 1) and (right): $A_{4,4}$ (media 2) which were captured at intervals along the beam's propagation.

In generating a superposition of two higher-order Bessel fields using our set-up, the ring slit aperture is divided equally in the radial direction to yield two ring slits. The Bessel field produced by each ring slit propagates with slightly differing wave vectors, and hence the superposition field is made up of modes with differing phase velocities. In such a situation one would expect the interference pattern of the modes to change during propagation. To see that this interference leads to a rotation of the field, consider the following superposition:

$$A_{m,-m}(r, \phi, z) = J_m(k_{1r}r) \exp(i(k_{1z}z + m\phi)) + J_{-m}(k_{2r}r) \exp(i(k_{2z}z - m\phi)) \quad (8)$$

where the wavevectors differ by an amount $\Delta k = k_{2z} - k_{1z}$. The expression in Eq. (8) may be written in the form:

$$A_{m,-m}(r, \phi, z) \sim J_m(k_r r) \exp(ik_{1z}z + m\phi) (1 + \exp[i(\Delta kz - 2m\phi)]), \quad (9)$$

from which we note that the intensity of the superposition is given by the following proportionality:

$$I_{m,-m}(r, \phi, z) \propto J_m^2(k_r r) (1 + \cos(\Delta kz - 2m\phi)). \quad (10)$$

Such a field experiences a rotation of its intensity pattern during propagation at a constant angular velocity, and at a rate along the propagation axis given by:

$$\frac{d\phi}{dz} = \frac{\Delta k}{2m}. \quad (11)$$

Figure 7 shows animations of rotating fields based on Eq. (10). The experimental observation of the rotation of the field, despite the absence of any OAM in the final field, is in agreement with that predicted theoretically [16].

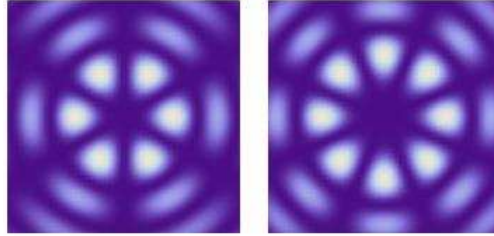


Fig. 7. Video clips containing theoretically calculated images for the rotation of fields (left): $A_{3,-3}$ (media 3) and (right): $A_{4,-4}$ (media 4).

By analyzing the experimental images recorded after the Fourier transforming lens, we can deduce the experimental propagation distance of the produced fields: 330 mm, 360 mm and 370 mm for the fields $A_{3,-3}$, $A_{4,-4}$, and $A_{2,-4}$ respectively; this is found to be in very good agreement with theory (~375 mm). The non-diffracting nature of the superposition fields can be understood from the fact that they are derived from the annular structure of the ring aperture, with the azimuthal phase only an additional degree of freedom. We report sans results that changing the dimensions of the ring slit aperture, as well as the focal length of the Fourier transforming lens, results in fields of differing non-diffracting propagation distances, as one might reasonably expect.

4. Conclusion

We have presented a technique to experimentally realize the superposition of higher-order Bessel beams, and demonstrated the superposition of both two and three higher-order Bessel beams, with the measured results in good agreement with the calculated fields. The propagation of these superposition fields was investigated, illustrating that these fields are propagation-invariant in accordance with prediction. The wavefront dislocations present in the higher-order Bessel beams were revealed by interferometric means, confirming the existence of higher-order vortices. These fields may aid the understanding of resonant transverse modes observed in certain laser resonators [17], and in optical trapping and tweezing for the control of micro-sized particles. In particular, in the case of generating a superposition of two higher-order Bessel beams which possess equal orders of azimuthal phase but of differing sign, the produced field carries no orbital angular momentum. Despite this, these beams are likely to be able to trap a particle in their intensity distribution and cause it to rotate over a spiral path along the beam's optical axis.

Finally, we would like to point out that the approach outlined here has not been optimized for energy transmission; the loss through the ring slit aperture is very high as may be expected. If this approach is to be followed in an application, then it would require a minor adjustment in set-up, for example, replacing the ring slit with a double axicon system to create the initial ring field.

Acknowledgements

We gratefully acknowledge the support from the National Research Foundation (Grant number 67432).